Korean J. Chem. Eng., 33(5), 1659-1668 (2016)
DOI: 10.1007/s11814-015-0298-1

pISSN: 0256-1115
eISSN: 1975-7220

Antibacterial and in vivo reactivity of bioactive glass and poly(vinyl alcohol) composites prepared by melting and sol-gel techniques

Salha Boulila[*,*,********], Hassane Oudadesse[*], Hafed Elfeki[***,†], Rim Kallel[**], Bertrand Lefeuvre[*], Mostafa Mabrouk[****], Slim Tounsi[*****], Dhekra Mhalla[*****], Amany Mostafa[****], Khansa Chaabouni[******], Fatma Makni-Ayedi[******], Allal Barroug[*******], Tahia Boudawara[**], and Abdelfattah Elfeki[********]**

*University of Rennes 1, UMR CNRS 6226, Campus de Beaulieu, 35042 Rennes, France
**Anatomopathology Laboratory, CHU Habib Bourguiba 3029, University of Sfax, Sfax, Tunisia
***Laboratory of Sciences Material and Environment, Faculty of Sciences of Sfax, B.P. 1171, Sfax 3000, Tunisia
****Refractories, Ceramics and Building Materials Department, National Research Centre, 33El Bohouth St. (Former EL Tahrir st.)- Dokki- Giza- P. O. 12622, Egypt
*****Biopesticides Team (LPAP), Centre of Biotechnology of Sfax, Sfax University, P. O. Box 1177, Sfax 3018, Tunisia
******Laboratory of Biochemical, University Hospital Habib Bourguiba, Avenue El Fardous, 3029 Sfax, Tunisia
*******University of Cadi Ayyad, Marrakech and CNRST Rabat, Maroc
********Laboratory of Animal Ecophysiology, Faculty of Sciences of Sfax, University of Sfax, P. O. Box 95, Sfax 3052, Tunisia
(*Received 13 September 2015 • accepted 28 December 2015*)

Abstract−Bioactive glass particle is used in the repair of bone defects. This material undergoes a series of surface *in vivo* reactions, which leads to osteointegration. We evaluated the effect of the bioactive glass synthesis, sol-gel (BG(S)) versus melting (BG(M)), associated with polyvinyl-alcohol (PVA) on *in vivo* bioactivity with biochemical parameters, liver-kidney histological structure and antibacterial *in vitro* activity. These composites were testified in many bacteria and implanted in ovariectomized rat. The serum and organs (liver and kidney) of all groups, control and treated rats, were collected to investigate the side effects of our composites, BG(S)-PVA and BG(M)-PVA, in comparison with control and ovariectomized rats. Also, the implants, before and after implantation, were prepared for analysis using physicochemical techniques such as Fourier transform infrared spectroscopy and X-ray diffraction. Our results have shown the stability of natremia, kaliemia, calcemia and phosphoremia. The histological structures of liver and kidney in implanted rats are intact compared to control and ovariectomized rats. BG(S)-PVA is characterized by a higher antibacterial effect on negative and positive gram bacteria than BG(M)-PVA. The physicochemical results have confirmed a progressive degradation of BG(S)-PVA and BG(M)-PVA, while replacing the implant by an apatite layer. But this bioactivity of BG(S)-PVA is faster than BG(M)-PVA. We can therefore confirm, on the one hand, the biocompatibility of our two implants and, on the other hand, the beneficial effect of sol-gel synthesis technique versus melting, both on the antibacterial effect and on the rapid formation of layer hydroxyapatite, and consequently on osteogenesis.

Keywords: Antibacterial, Bioactivity, Biocompatibility, Bioactive Glass, Melting, Sol-gel

INTRODUCTION

Tissue engineering is a promising field of bone repair and regenerative medicine in which cultured cells, scaffolds and osteogenic inductive signals are used to regenerate tissues. And with increasing population, there is a clinical demand for engineered bone tissue. One of the current challenges in tissue engineering is the development of suitable scaffold materials that can be used as templates for cell adhesion, growth and proliferation [1].

As demonstrated by Hench et al., a bioactive implant is among the materials that elicit a specific biological response at the interface of the material, which results in the formation of a bond between the tissues and the material. It has been reported that glass compositions in the SiO_2-CaO-Na_2O-P_2O_5 system are able to develop an apatite-like layer similar to bone mineral at the interface with body fluids [2] This is done by exerting control over the genetic factors of bone growth [1]. The level of bioactivity that is the rate of apatite layer formation and the apatite-like layer thickness is influenced not only by the product composition [2], but also by synthesis routes: melting versus sol-gel. The materials prepared by the sol-gel method have special mesoporous structure, which leads to specific enlarged areas and accelerated ion exchange rate between the material and surrounding medium [2]. One approach to enhance the mechanical properties of materials is the elaboration of bioactive glass-polymer composites. In fact, they often show an excellent combination between strength and toughness and improved characteristics, when compared to their individual components.

Among several choices of polymers, polyvinyl alcohol (PVA), a hydrophilic semicrystalline polymer, has been frequently explored as an implant material in a wide range of biomedical applications

†To whom correspondence should be addressed.
E-mail: hafedelfeki@yahoo.com

such as drug delivery systems, wound dressings, membranes, surgical repairs, artificial skin [3], tissue scaffolding [4], artificial cartilage [5] and biodegradable scaffolds [6], mainly due to its excellent mechanical strength, biocompatibility, and nontoxicity [3].

Generally, the dissolution rate and microbial infection of implants/biomaterials in orthopedic surgery are still critical health concerns. Infections associated with orthopedic surgery are usually caused by Gram-positive organisms such as *Staphylococcus aureus*, *S. epidermidis*, and streptococci and Gram-negative organisms such as *Escherichia coli*, *Enterobacter* and *Pseudomonas aeruginosa*. An ideal bone substitute should be osteogenic, biocompatible, and resorbable. It should not only be capable of giving structural support, preventing biofilm formation, and serving as a drug carrier, but also easy to use clinically [7]. Furthermore, it is used for minimizing the danger of infection, risk of implant failure, and even avoiding patient death [8]. Previous studies have shown that antibacterial biomaterials are increasingly being considered as a main strategy to prevent infections [9] by developing a BG with an optimal concentration of silver [10], fluoride [9] or zinc [11]. In this case, BG is used as a support for the agent controllable release [12]. Mortazavi et al. [7] demonstrated that certain bioactive glasses exhibit antibacterial activity. This may result from one of the surface reactions undergone by these glasses [7]. There is commonly a good correlation between the results of cell cultures and *in vivo* studies. But because of the complexity of the human body, there may be exceptions and damage to the tissue *in vivo*. That is why it is essential to test the material on animals before it is introduced into the body of a human.

Our aim here was to determine the effect of exposure to two biocomposites composed of a bioactive glass. These biocomposites were synthetized by melting and sol-gel and associated with biodegradable polymer (PVA) on the viability of a range of bacteria *in vitro*. In vivo biocompatibility, degradability and bone forming capacity of the composites were studied using ovariectomised rats as osteoporotic model.

MATERIALS AND METHODS

1. Fabrication of BG(M)-PVA Composite

The 46S6 bioactive glass was prepared as previously reported [13] by using calcium silicate (Alfa Aesar), trisodium trimeta phosphate and sodium metasilicate pentahydrate (Sigma). The prepared glass was named BG(M). Bioactive glass(melting)-polyvinyl alcohol (BG(M)-PVA) in molar ratio 2 : 1. BG(M)-PVA scaffolds was prepared by employing thermally-induced phase separation technique (freeze drying). Firstly, 15% of PVA (Aldrich, Mwt=67.000) was dissolved in distilled water at 80 °C for 2 hours. The prepared glass BG(M) was added to polymer solution with continuous stirring at room temperature for 20 hours [14].

2. Fabrication of BG(S)-PVA Composite

46S6 bioactive glass powder was synthesized by sol-gel method BG(S) as follows. A colloidal solution of 46S6 was prepared by sol-gel. Initially, 56 ml of tetraethoxysilane (TEOS: Fluka, Mwt=208.33) was added to 350 ml of distilled water and 350 ml of ethanol at room temperature. PH was adjusted at 2 by nitric acid with continuous stirring for 1 h. We added 24.5 g of calcium nitrate hydrate (Fluka, Mwt=236) to the above solution, while stirring continuously till dissolving. After the addition of 21.07 g of sodium hydroxide (Prolab, Mwt=40) to the above mixture (the previous mixture was named solution A), 10 g of polyethylene glycol (PEG-Fluka Mwt=600) was dissolved in 400 ml of distilled water at room temperature. An amount of 3.43 g of ammonium dihydrogen phosphate (MERK, Mwt=115.03) was added to the PEG solution, which was termed solution B. Furthermore, solution B was gradually added to solution A with continuous stirring overnight. The resulting solution was filtered and washed with distilled water three times and with ethanol once using centrifuge with 1,650 rpm for 10 min drying of the washed gel at 70 °C overnight. The dried powder was calcined at 600 °C for two hours. PVA (ALDRICH, Mwt= 67.000) was dissolved in distilled water at 80 °C for two hours using a polymer concentration of 15 wt%. BG(S)-PVA was in molar ratio 2 : 1. BG(S) was added to the PVA solution with continuous stirring for overnight using a magnetic stirrer to break the BG agglomerates and ensure a better (homogeneous) distribution of BG(S) particles in the composite scaffolds [3].

3. Animal Model

Female Wistar rats, with body weights from 250 to 300 g bred in the central animal house and obtained from the central pharmacy of Tunisia, were used in this study. The animals were fed on a pellet diet (Sicco, Sfax, Tunisia) and water ad libitum. The animals were maintained in a controlled environment under standard conditions of temperature (22±2 °C) and humidity (55±5%) with an alternating light-and-dark (12/12 hours) cycle, and acclimatized for one week prior to the start of the experimentation. They were divided into four groups of 20 rats each:

- Group (I): Used as negative control (T); without ovariectomy and the femoral condyles were intact and without a surgical creation of bone defects.

Sixty days after bilateral ovariectomy, the rats developed the bone disorder, and thus could be used as the animal model for osteoporosis.

- Group (II): Used as positive control (T^+); with ovariectomy and without a surgical creation of bone defects.
- Group (III); Sixty days after bilateral ovariectomy, the bone defects were implanted with BG(M)-PVA.
- Group (IV); Sixty days after bilateral ovariectomy, the bone defects were implanted with BG(S)-PVA.

4. Surgical and Postoperative Protocol

BG(M)-PVA and BG(S)-PVA powder was sterilized, implanted and stabilized in femorale condyle. Anaesthesia was induced with chloral hydrate depending on body weight. A drilled hole, 4 mm in diameter and 5 mm in depth, was created aseptically and the pellets filled the loss of osseous substance only for the third (BG(M)-PVA) and fourth (BG(M)-PVA) groups. During the period of treatment, the subjects were checked daily for clinical complications. On days 15, 30, 60 and 90 after implant insertion, the rats were sacrificed and specimens (serums, organs and implants) were stored for subsequent biological and physicochemical evaluations. The handling of the animals was approved by the Tunisian Ethical Committee for the care and use of laboratory animals.

5. Biochemical Analysis

The serum levels of Calcium (Ca), Phosphorus (P), Sodium

(Na) and Potassium (K) were measured in frozen aliquots of serum by standardized enzymatic procedures using commercial kits from (Biolabo, France) on an automatic biochemistry analyzer (Vitalab Flexor E, USA) at the clinic pathological laboratory of Habib Bourguiba Hospital (Sfax, Tunisia).

6. Histological Studies

Liver and kidney samples were fixed in 10% of formalin and processed in a series of graded ethanol solutions. They were then embedded in paraffin, serially sectioned at 5 mm and stained with hematoxylin-eosin (H-E) examined by light microscopy.

7. Agar-well Diffusion Assay

The antimicrobial activities of different extracts of leaves were evaluated by means of agar-well diffusion assay. The microorganisms of standardized cultures (100 µl) were spread onto the surface of agar plates. Then, wells of 6 mm in diameter were punched in the inoculated agar medium with sterile Pasteur pipettes and 50 µl of the extracts were added to each well at concentrations of 100 mg/mL. The extracts underwent diffusion in the plate for 2 h at 4 °C. The agar plates were incubated at 30 °C for 24 h for bacterial strains. The antimicrobial activity was evaluated by measuring the zones of inhibition (clear zone around the well) against the test micro-organisms.

8. Physicochemical Analysis

The implant samples were characterized by X-ray-diffraction (XRD) and Fourier transform infrared spectroscopy (FTIR). The XRD pattern of powder samples was measured on a D8 Bruker diffractometer controlled by an IBM PC microcomputer. It was used to analyze the structure of the prepared BG(M)-PVA and BG(S)-PVA before and after implantation. The diffractometer was operated at 40 kV and 30 mA at 2θ range of 10-70°.

FTIR (Nicolet Magna-IR 550 spectrometer, Madison, Wisconsin) was performed to identify the nature of the chemical bonds between atoms. The samples were small pellets, of 0.5 cm in diameter, obtained by pressing the scaffold powder with KBr [14]. The IR spectra were in the 4,000-400 cm^{-1} range using Opus software.

9. Statistical Analysis

The data were analyzed using the statistical package program Stat view 20 Soft Ware for Windows (SAS Institute, Berkley, CA). Statistical analysis was performed using one-way analysis of variance (ANOVA) followed by Fisher's protected least significant difference (PLSD) test as a post-hoc test for comparison between groups. All values were expressed as mean±SE. Differences were considered significant if $p<0.05$.

RESULTS AND DISCUSSION

1. Physicochemical Parameters

1-1. X-ray Diffraction Results

The results of the X-ray diffraction analysis from the pure bioactive glass synthesized by melting (Fig. 1) and sol-gel (Fig. 2) were as expected. Actually, they did not show the presence of any crystalline phase, being totally amorphous with a hump at 32°. The PVA also presented an amorphous structure and had a hump at 20°. The association between BG(M) and PVA, on the one hand, and BG(S) and PVA, on the other hand, showed the same structure type, with two humps at 20 and 32°. It highlights the chemical interactions between bioactive glass and PVA polymer which induces the changes in the glass amorphous structure.

The XRD patterns for BG(M)-PVA and BG(S)-PVA after implantation into the femoral condyle for ovariectomized rats, in different periods (15, 30, 60 and 90 days) with reference to hydroxyapatite synthesis model are shown in Figs. 1 and 2, respectively. Fig. 1 shows that, after 15 and 30 days of implantation, the diffraction pattern of the BG(M)-PVA implant in the site of the femoral condyle has three lines, observed at 26°, 32° and 40° (2θ). These lines correspond to the reflection planes (002), (211) and (310) of

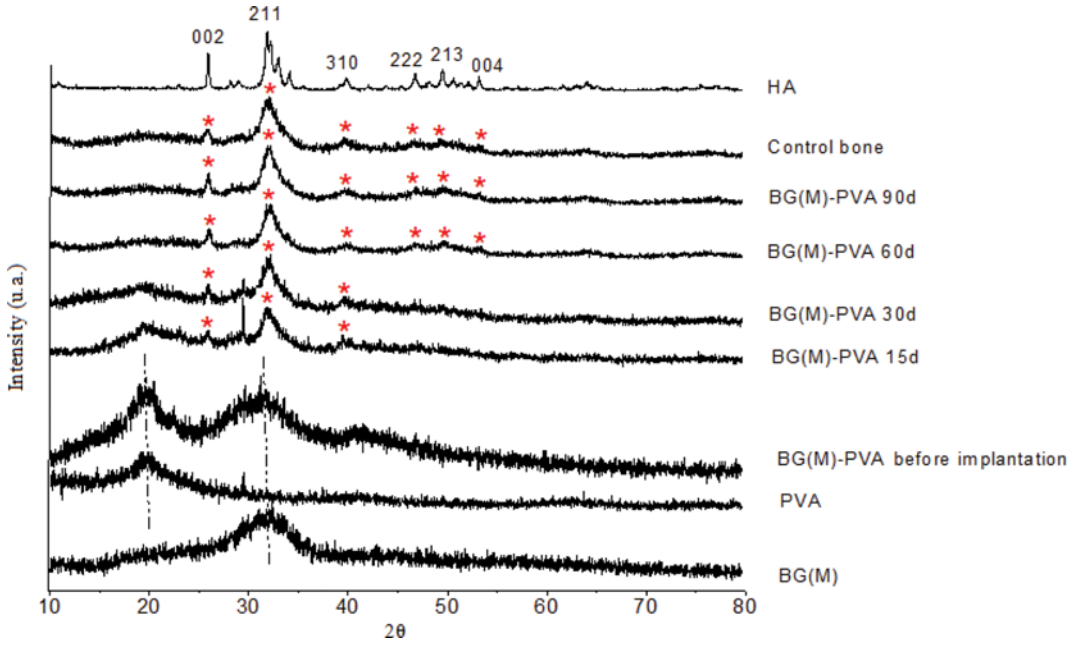

Fig. 1. Diffractogramm of BG(M)-PVA before and after implantation (15, 30, 60 and 90d).

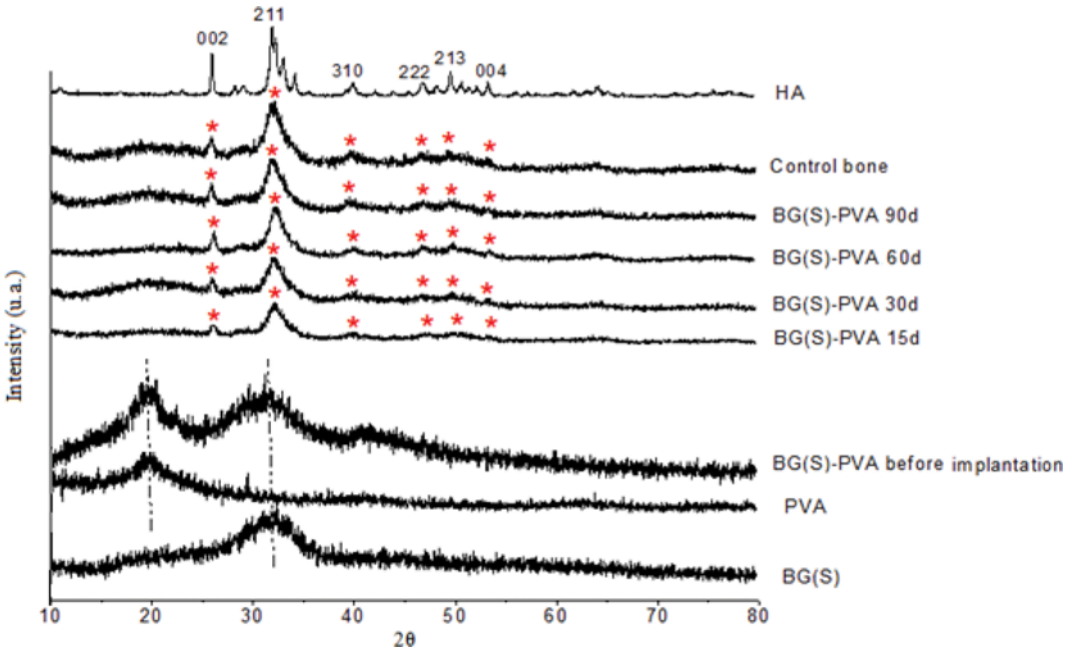

Fig. 2. Diffractogramm of BG(S)-PVA before and after implantation (15, 30, 60 and 90d).

hydroxyapatite crystals, respectively. It is to be noted that the line 211 corresponds to the hump already observed in the diffractogram BG(M)-PVA before implantation, which confirms the formation of the hydroxyapatite layer.

After 60 and 90 days of implantation, the intensities of the peaks at 26° (002), 32° (211) and 40° (310) increase slightly. Three further lines were also observed approximately at 47°, 50° and 53°, corresponding to the reflection plane (222), (213) and (004) of apatitic phase, respectively. This gives birth to a new apatite phase and the improvement of its crystallization as a function of time of implantation. However, the formation of apatitic layer of BG(S)-PVA is faster than that of BG(M)-PVA with a more improved crystallinity, which is in agreement with the work of Gao et al. [15].

After 15 days of implantation, six peaks characterizing hydroxyapatite (HA) were observed at 26° (002), 32° (211), 40° (310), 47° (222), 50° (213) and 53° (004) for the BG (S)-PVA sample (Fig. 2). The intensity and degree of crystallinity of these peaks increase with the increase in implantation time; otherwise after 30, 60 and 90 days, the apatitic layer has a very high crystallinity. This confirms the higher reactivity of the glass sample prepared by the sol-gel than that prepared by the melting method. In fact, the incorporation of BG(S) into PVA polymer enhances the compressive strength, due to their small particle size and large surface area, which results in great attachment of BG(S) particles to the polymer matrix [3,16-19]. The sol-gel method enables the production of glasses with enhanced bioactivity, compared to melt-derived glasses with the same composition thanks to its highly porous nature [20].

Other studies have shown that sol-gel glasses prepared within three (SiO_2-CaO-P_2O_5) and two (SiO_2-CaO) component systems, and even pure silica, can quickly develop an apatite layer in contact with simulated body fluids [20-23]. Bone-like apatite was formed at the glass surface prepared by sol-gel route after 2 hours. However, the formation of this apatite was delayed to 1 day when the glass was prepared by melting method [2]. BG(S) exhibits a greatly higher specific surface area and pore volume than BG(M). These parameters may be a key factor of glass bioactivity. *In vitro*, the high porosity in BG(S) favors the formation of the bone-like apatite layer, as it facilitates the rapid and considerable release of Ca^{2+} ions from the glass to the solution. BG(S) shows that the ionic products such as Si and Ca strongly influence the proliferation of osteoblasts, thus inducing bone growth. Moreover, the mineralization of the bone must be done with the transport of P, which in turn depends on the dissolution of Na.

Previous studies have proven that the quantitative analysis of the prepared powder samples BG(S) and BG(M) is determined by X-ray fluorescence spectrometry (XRF). It is obvious that the two samples have the same chemical composition with small fractions of impurities (0.892% for BG(M) and 0.406% for BG(S)). This means that BG(S) has fewer impurities than BG(M). Therefore, the prepared 46S6 bioactive glass by sol-gel method has a high purity and can be considered good for cell viability. Then, this synthesis method is effective for preparing bioactive glass nanopowder BG(S) as a bone replacement material [1]. With the progression time of implantation, for BG(S)-PVA and BG(M)-PVA, peaks close to the normal bone were obtained. The crystallization of apatite is the final stage and is considered important in the multistep process of the hard tissue formation [24,25]. Thus, as a function of time, the BG(S)-PVA and BG(M)-PVA are crystallized successively to layer hydroxyapatite. In addition, the osteoinduction bioactive glass may come from the products of its dissolution into the biological environment [26].

1-2. Fourier Transform Infrared Spectroscopy Results

Figs. 3 and 4 show the IR spectra of BG(M)-PVA and BG(S)-PVA biocomposites before and after implantation. The spectrum of bioactive glass (before implantation), synthesized by melting and sol-gel shows the characteristic bands of silica network. It

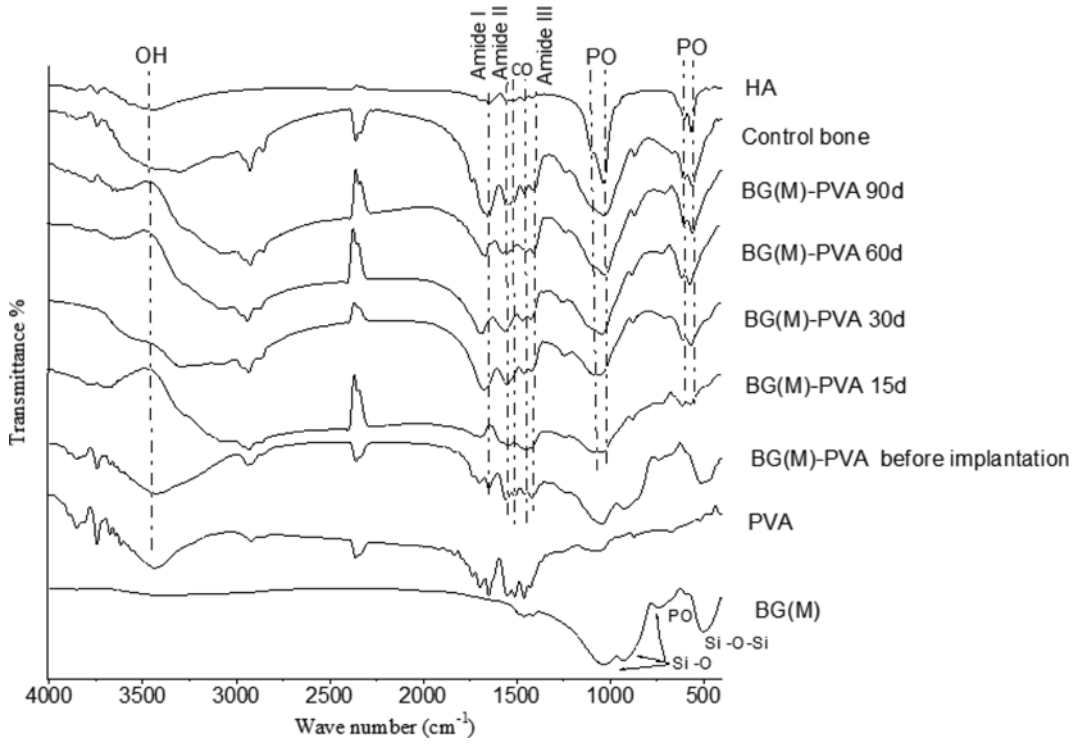

Fig. 3. Spectrum of BG(M)-PVA before and after implantation (15, 30, 60 and 90d).

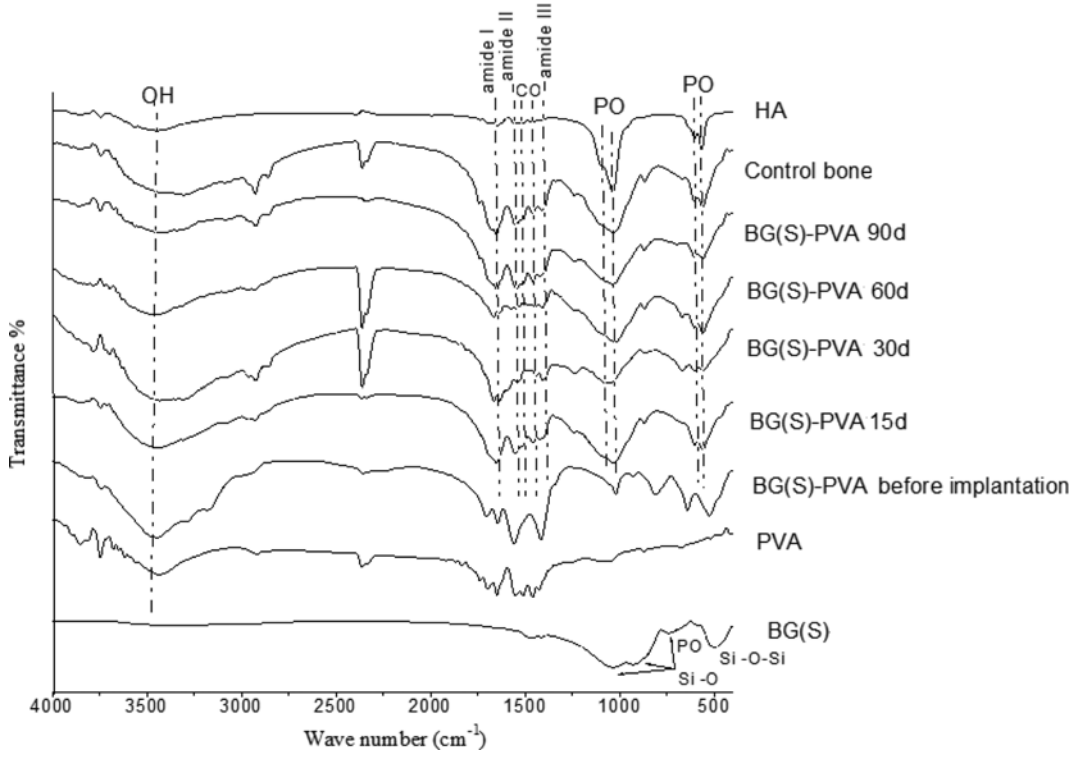

Fig. 4. Spectrum of BG(M)-PVA before and after implantation (15, 30, 60 and 90d).

reveals four broad absorption bands. The first band at about 498 cm^{-1} is characteristic of the angular deformation vibration of Si-O-Si bond between SiO_4 tetrahedrons in silicate network. Three other characteristic bands at 745, 925 and 1,034 cm^{-1} attributed to the stretching vibrations of Si-O bond in each SiO_4 tetrahedron are detected. In addition, only a slight band at 600 cm^{-1} is characteris-

tic for the bending vibration of O-P-O group. It reveals the presence of a small quantity of phosphate related to the silica network. It is possible that other modes of vibration of the PO_4 groups appear except that they are superposed with the modes of vibration of Si-O.

The IR spectrum of PVA proves the presence of "OH" group peak of alcohol at 3,430 cm^{-1}, which is assigned to the stretching vibration of OH group due to the strong hydrogen bond of intramolecular and intermolecular type [3,25]. Besides, the band at 2,924 cm^{-1} is attributed to the alkyl stretching mode (νCH). The bands ranging from 1,700 to 1,736 cm^{-1} and 1,208-1,294 cm^{-1} arise due to the stretching vibration of carbonyl (νC=O) and ester, respectively, from the vinyl acetate group found in partially hydrolyzed PVA polymer. Some other bands which can be found related to PVA are located at 1,425-1,548 cm^{-1} assigned to δ(CH)CH_2.

The IR spectrum of BG-PVA biocomposite before implantation shows the characteristic bands of both PVA and bioactive glass. However, several characteristic bands are shifted, deformed or disappeared. This is attributed to some chemical interactions between the bioactive glass and the PVA. Note that the composite formation leads to the broadening of the bands related to vinyl acetate copolymer that almost disappears as a consequence of the hydrogen bonds involving CO groups and silanol groups in silicate networks [3,27]. The same results are obtained for the two implants: (BG(M)-PVA and BG(S)-PVA).

After 15 days, two characteristic bands of Si-O bond of BG at 928 and 1,034 cm^{-1} completely disappeared. The other bands were slightly modified. The characteristic bands of the apatite phase started to appear but were more significant in BG(S)-PVA than BG(M)-PVA. The IR spectrum of the BG(S)-PVA implant shows the characteristic bands of crystalline phase of hydroxyapatite, which is more important than in BG(M)-PVA. Three new bands P-O (565, 607 and 1,034 cm^{-1}) are observed for the two implants. They are characteristic of phosphates PO_4^{3-} crystalline phase. In addition, the bands characteristic of carbonate (CO_3^{2-}) at 868 and 1,461 cm^{-1} are also present in BG(S)-PVA and BG(M)-PVA. They are characteristic of the bending vibration and elongation of the CO bond in the CO_3^{2-} group. These results confirm the formation of a carbonated hydroxyapatite layer following the implantation of our composites, which is in agreement with that found in other studies [25,28]. Then, these *in vivo* results pointed to the bioactivity of our composites by the creation of a new bone, confirming their ability to support the invasion of cells (osteoblasts). The characteristic bands of the apatite layer became more significant after 30, 60 and 90 days of implantation. In fact, there are displacements of most of the bands mentioned previously. The bands attributed to amide I, II and III appeared at 1,650, 1,549 and 1,411 cm^{-1}, respectively, which is very near to the control bone structure. This result confirms that the crystallization of the apatite layer formed on the surface of the implant increases with the period of implantation. Therefore, the high bioactivity of BG(S)-PVA is due to the synthesis method because the sol-gel presents a more superior reactivity *in vivo* than in melting, which confirms the X- ray results.

2. Biochemical Parameters

In our study, serum sodium (Fig. 5), potassium (Fig. 6) calcium (Fig. 7) and phosphore (Fig. 8) in the groups implanted by BG(M)-PVA and BG(S)-PVA show no significant variation for all periods of implantation, compared to ovariectomized rats (T+) and control (T). Therefore, these composites do not cause side effects to all implanted groups. This is a beneficial result due to their biocompatibility.

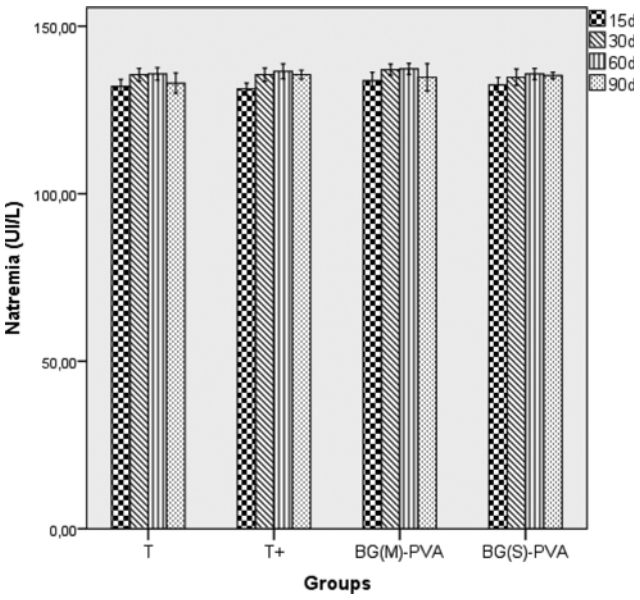

Fig. 5. Variation of natremia level in different groups controls and implantated. Data represent mean +/− standart deviation.

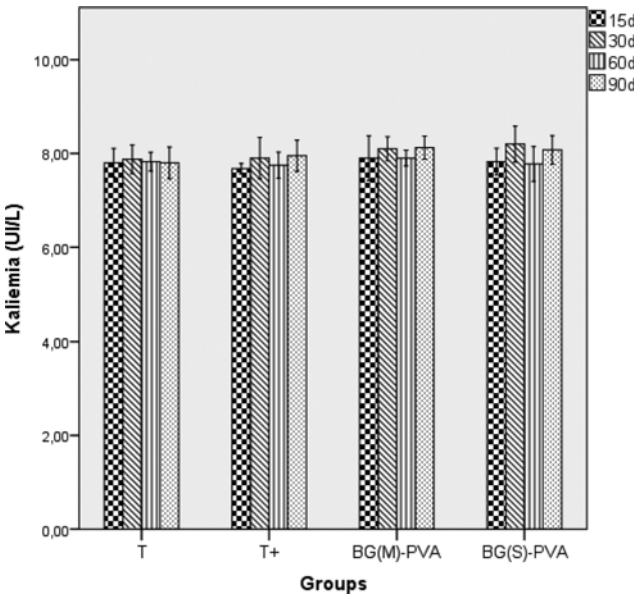

Fig. 6. Variation of kaliemia level in different groups controls and implantated. Data represent mean +/− standart deviation.

Other research works have shown that, in the blood plasma of ovariectomized rats implanted by bioactive glass, P and Ca content is normal [25]. Thus, due to the biocompatibility and osteogenic capacity of bioactive glass, it came to be known as "bioactive glass" [29]. The physiopathology of primary osteoporosis is marked by reduced bone density but without any significant change in

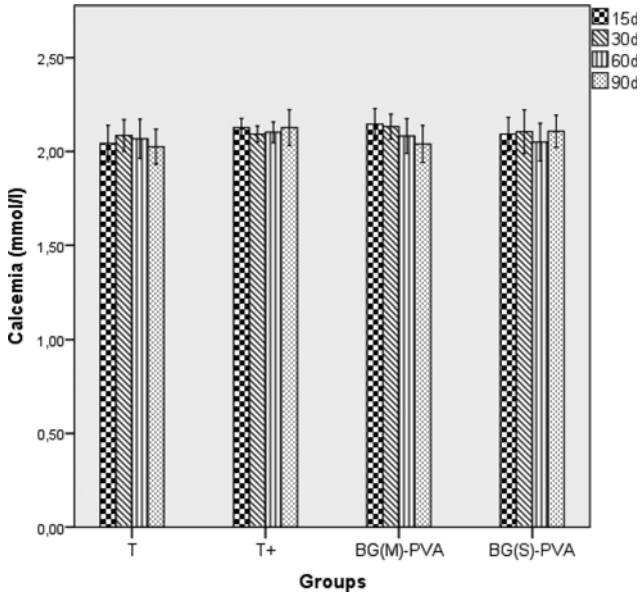

Fig. 7. Variation of calcemia level in different groups controls and implantated. Data represent mean +/− standart deviation.

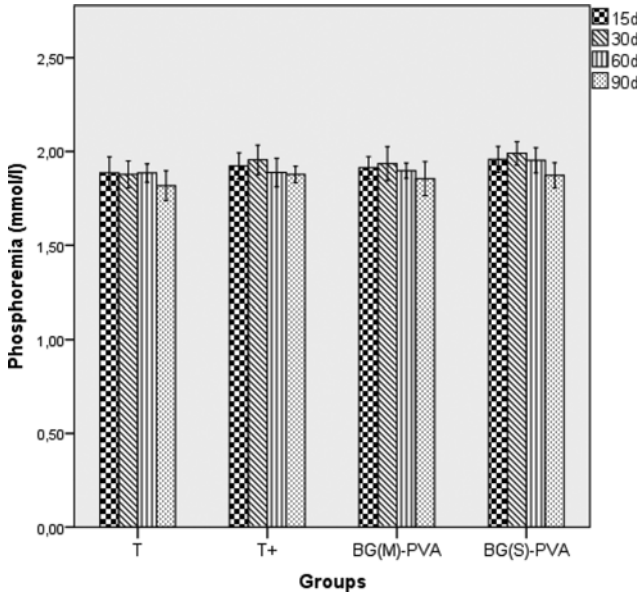

Fig. 8. Variation of Phosphoremia level in different groups controls and implantated. Data represent mean +/− standart deviation.

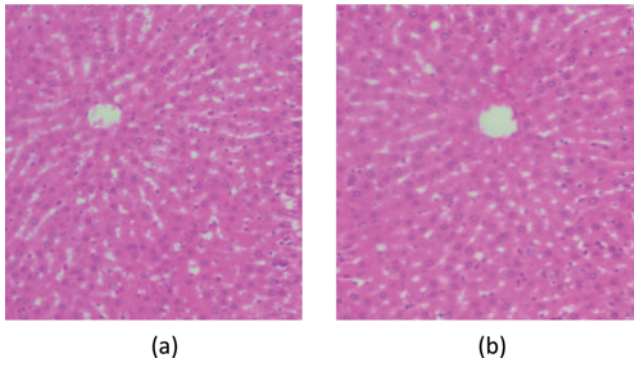

Fig. 9. Photomicrographs showing histological of liver in control rats (T), after 15 (a) and 90 (b) days of implantation, evaluated by haematoxylin and eosin (H-E) staining (100×).

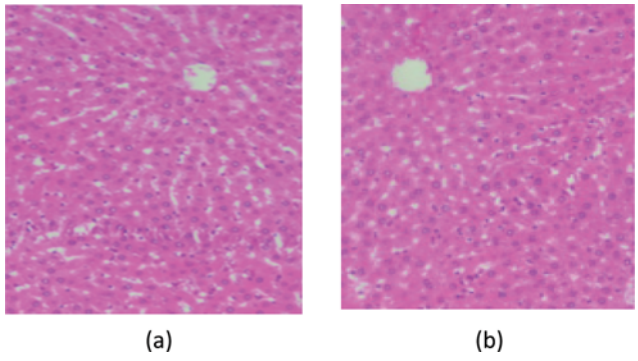

Fig. 10. Photomicrographs showing histological of liver in ovariectomised rats (T+), after 15 (a) and 90 (b) days of implantation, evaluated by haematoxylin and eosin (H-E) staining (100×).

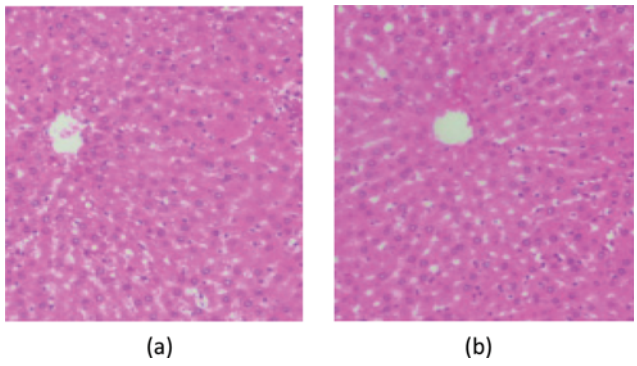

Fig. 11. Photomicrographs showing histological of liver in implanted rats with BG(M)-PVA, after 15 (a) and 90 (b) days of implantation, evaluated by haematoxylin and eosin (H-E) staining (100×).

phosphocalcic blood parameters [30].

3. Histological Studies

3-1. Liver Observations

In recent decades, many biomaterials for bone tissue engineering have been examined with respect to their biocompatibility [31]. The histological sections of liver controls (T), ovariectomized (T+) and implanted (BG(M)-PVA and BG(S)-PVA) have a normal structure (Figs. 9, 10, 11 and 12). The structural units of the liver are called liver lobules. These lobules are separated from each other and sharply delimited by a layer of connective tissue. It is a hexagonal mass of tissue primarily composed of plates of hepatocytes that radiate from the region of the central vein (present in the center) toward the periphery. The plates are separated by hepatic sinusoids. The arterial and venous blood flows centripetally in each lobule (from the portal areas to drain in the central vein), whereas the bile flows centrifugally towards the portal areas. This is the centrolobular zone, which is composed of hepatocytes surrounding the central vein, and the most distant zone from the

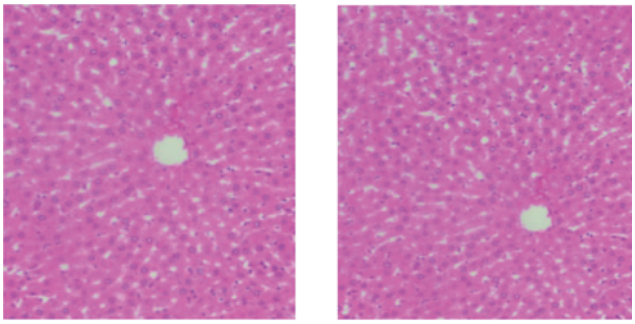

Fig. 12. Photomicrographs showing histological of liver in implanted rats with BG(S)-PVA, after 15 (a) and 90 (b) days of implantation, evaluated by haematoxylin and eosin (H-E) staining (400×).

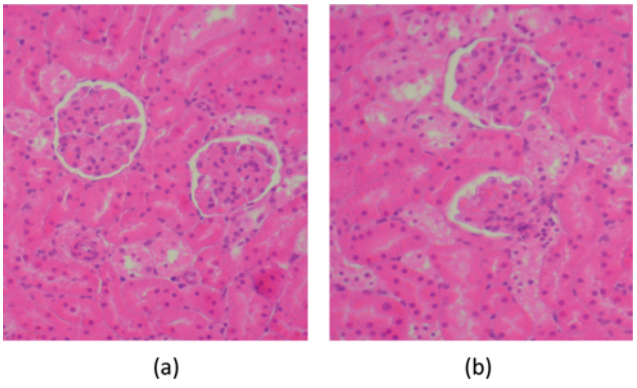

Fig. 13. Photomicrographs showing histological of kidney in control rats (T), after 15 (a) and 90 (b) days of implantation, evaluated by haematoxylin and eosin (H-E) staining (400×).

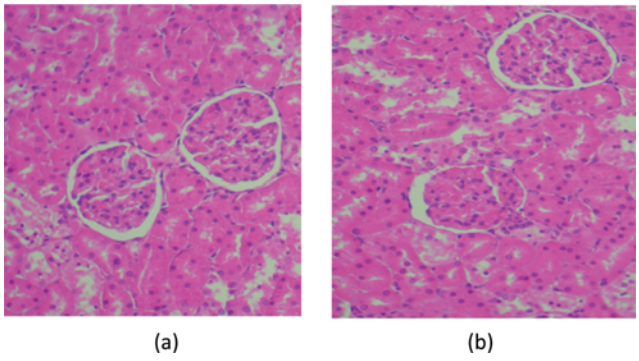

Fig. 14. Photomicrographs showing histological of kidney in ovariectomised rats with (T+), after 15 (a) and 90 (b) days of implantation, evaluated by haematoxylin and eosin (H-E) staining (400×).

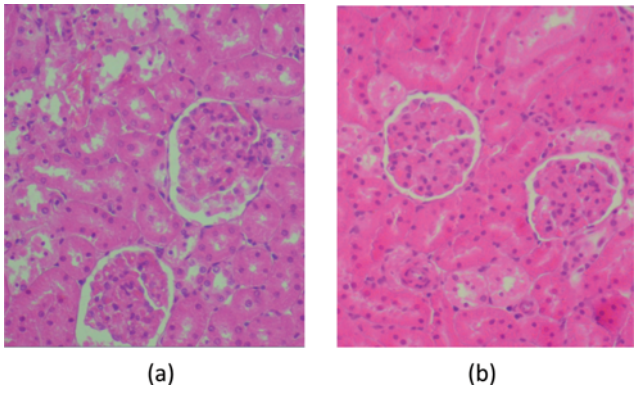

Fig. 15. Photomicrographs showing histological of liver in implanted rats with BG(M)-PVA, after 15 (a) and 90 (b) days of implantation, evaluated by haematoxylin and eosin (H-E) staining (400×).

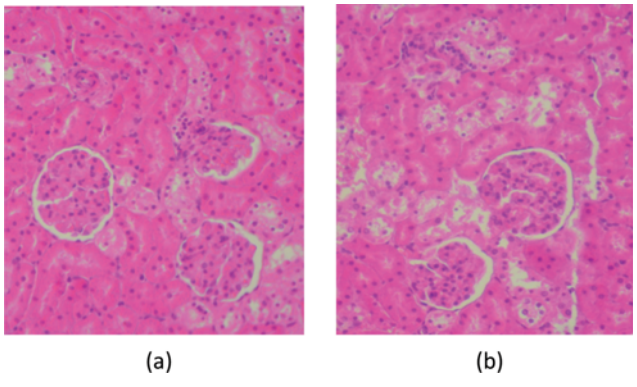

Fig. 16. Photomicrographs showing histological of liver in implanted rats with with BG(S)-PVA, after 15 (a) and 90 (b) days of implantation, evaluated by haematoxylin and eosin (H-E) staining (400×).

oxygenated arterial blood supply. Since no necrotic lesions were noted, our implants do not have side effects on the liver histoarchitecture after 15 and 90 days of implantation, and consequently present a high biocompatibility. If the materials are biodegradable, their degradation products should not be toxic and should not provoke an adverse immune response. Among the developed biomaterials for bone tissue, composite materials containing both inorganic phases (glass and polymer) are considered an optimal approach [31].

3-2. Kidney Observations

Furthermore, our kidney sections of various groups T, T+, BG(M)-PVA and BG(S)-PVA have neither nephritis or extensive infiltrates (Figs. 13, 14, 15 and 16). Each nephron consists of a tuft of anastomosing capillaries called the glomerulus, formed from the afferent arteriole and draining into the efferent arteriole, and a tubular system called the renal tubule. Epithelial cells called podocytes (orvisceral epithelium of Bowman's capsule) invest the glomerulus, and are reflected to become continuous with the parietal epithelium of the Bowman's capsule. Bowman's capsule is the bulbous, distended, closed proximal end of the tubular system and is invaginated by the glomerulus. Therefore, our implants do not cause any signs of renal toxicity, after 15 and 90 days of implantation, which confirms their biocompatibility. The resorption of bioactive glass is affected by the ionic dissolution of Na, Ca, P and Si, which is necessary to the human body and is biologically regulated. Knowing that the polyvinyl alcohol (PVA) is nontoxic [32],

Table 1. Effect of BG(M)-PVA and BG(S)-PVA on many bacteria (Positive and negative gram) by measuring the diameter en mm

		BG(M)-PVA	BG(S)-PVA
Positive gram	*Bacillus subtilis*	10±1	15±1
	Bacillus cereus	12±1	18±1
	Staphylococcus aureus	9±1	15±1
	Micrococcus luteus	8±1	16±1
Negative gram	*Escherichia coli*	9±1	12±1
	Klebsiella pneumoniae	10±2	13±1.5

Data represent mean±SD

it has recently been tested as an engineering scaffold and drug delivery system [33].

4. Antibacterial Activity

To validate and verify the antibacterial effectiveness of our composites, various bacteria were used in our test. Table 1 shows the tendency of BG(M)-PVA and BG(S)-PVA to acquire antibacterial activity *in vitro* with diferent effects. Our choice is based on two types of Gram-positive (*Bacillus subtilis*, *Bacillus cereus*, *Staphylococcus aureus*, *Micrococcus luteus*) and negative bacteria (*Escherichia coli*, *Klebsiella pneumoniae*), because of their broad involvement in the contamination and infection of the phenomena encountered in the medical domain and particularly orthopedic field. While BG(M)-PVA has an antibacterial effect on Bacillus subtilis, Bacillus cereus and Klebsiella pneumoniae, BG(S)-PVA is shown to have an effect on all tested bacteria. Indeed, Bacillus subtilis, Bacillus cereus and Klebsiella pneumoniae have a higher sensitivity to BG(S)-PVA than BG(M)-PVA.Therefore, BG(S)-PVA causes a significant reduction in bacterial viability and consequently is characterized by a more significant antibacterial effect than BG(M)-PVA.

Echezarreta-López et al. [34] pointed out the utility of the antibacterial activity of BG in oral, orthopedic implants and wound dressings [34]. Our results are confirmed by the work of Mortazavi et al. [7] which showed that bioactive glass nanopowders, synthesis by sol-gel, could be considered as good candidates for the treatment of oral bone defects and root canal disinfection [7]. An interesting technique to diminish the bacteriological risks associated with different sorts of infections is the local release of specific ions into the body. In this technique, the glass network could act as a suitable carrier for the controllable release of different agents such as fluoride-containing bioactive glass as a novel scolicidal agent to prevent post-surgery infections, especially hydatidosis [12]. The antibacterial action of a bioactive glass is affected by its chemical composition and the dissolution conditions in its surroundings. It has been shown that the antibacterial effect of bioactive glass could be greatly improved by decreasing its particle size, and therefore by the immediate release of alkaline species such as calcium, phosphate, and silicate in the culture medium, thereby increasing pH level and inducing osmotic effects [7].

In general, all articles reviewed consider that the variation of environmental pH is a critical parameter for the antimicrobial activity of bioactive glasses [34]. This may reduce the bacterial colonization of its surface *in vivo* [35]. But in our study, it is strictly related to the synthesis method with the same chemical composition. Differences in BG antimicrobial activity regarding its production method have been extensively referenced in the literature, the sol-gel method being the best in producing high porosity particles and increase in the surface area that promotes higher ion release to the medium [7,21,34]. In our study, we tested our composite (BG(S)-PVA and BG(M)-PVA) on negative and positive bacteria. The susceptibility of species to antimicrobial agents varies according to the presence or absence of a lipopolysaccharide layer (Gram-negative or Gram-positive) in their cellular wall and their kind of association and growth, or their biofilm formation capacity, which is different as in coccus and bacillus [7,34,36,37]. The structural organization of the lipopolysaccharide layer gives bacteria resistance against BG [34,37,38].

CONCLUSION

The obtained biological studies have shown that the composites derived from melting and sol-gel are biocompatible *in vivo* and they cause neither biochemical nor histological perturbation. From the antimicrobial activity *in vitro* and physicochemical results, the material is more reactive when it is prepared by sol-gel method. It is concluded that BG(S)-PVA could be a potential candidate for tissue engineering applications because of its excellent *in vitro* antimicrobial and *in vivo* bioactivity properties in comparison with BG(M)-PVA. Thus, the sol-gel method reduces the bacteria viability, on the one hand, and enhances the bioactive glass resorption associated with PVA, on the other hand. The combined results highly recommend the implementation of the prepared composites in the evolution of biomaterials for bone tissue regeneration.

REFERENCES

1. M. Mabrouk, A. Mostafa, H. Oudadesse, E. Wers, A. Lucas-Girot and M. I. El-Gohary, *Bioceram. Dev. Appl.*, **4**, 1000072 (2014).
2. F.-Z. Mezahi, A. Lucas-Girot, H. Oudadesse and A. Harabi, *J. Non-Cryst. Solids*, **361**, 111 (2013).
3. M. Mabrouk, A. A. Mostafa, H. Oudadesse, A. A. Mahmoud and M. I. El-Gohary, *Ceram. Int.*, **40**, 4833 (2014).
4. F. E. Wiria, C. K. Chua, K. F. Leong, Z. Y. Quah, M. Chandrasekaran and M. W. Lee, *J. Mater. Sci. Mater. Med.*, **19**, 989 (2008).
5. Y. Pan and D. Xiong, *Wear*, **266**, 699 (2009).
6. M. Wang, Y. Li, J. Wu, F. Xu, Y. Zuo and J. A. Jansen, *J. Biomed. Mater. Res. A*, **85**, 418 (2008).
7. V. Mortazavi, M. M. Nahrkhalaji, M. H. Fathi, S. B. Mousavi and B. N. Esfahani, *J. Biomed. Mater. Res. A*, **94**, 160 (2010).

8. M. Mozafari and F. Moztarzadeh, *Int. Ceram. Rev.*, **62**, 423 (2014).
9. M. Gholipourmalekabadi, M. Sameni, A. Hashemi, F. Zamani, A. Rostami and M. Mozafari, Silver- and fluoride-containing mesoporous bioactive glasses versus commonly used antibiotics: Activity against multidrug-resistant bacterial strains isolated from patients with burns, *Burns* (2015).
10. M. Mozafari, *Bioceram. Dev. Appl.*, **4**, e106 (2014).
11. F. Baghbani, F. Moztarzadeh, L. Hajibaki and M. Mozafari, *Bull. Mater. Sci.*, **36**, 1339 (2014).
12. A. Rostami, M. Mozafari, M. Gholipourmalekabadi, H. H. Caicedo, Z. Lasjerdi, M. Sameni and A. Samadikuchaksaraei, *Acta Trop.*, **148**, 105 (2015).
13. E. Dietrich, H. Oudadesse, A. Lucas-Girot and M. Mami, *J. Biomed. Mater. Res. A*, **88**, 1087 (2009).
14. M. Mabrouk, A. A. Mostapaha, H. Oudadesse, A. A. Mahmoud, A. M. Gaafar and M. I. El-Gohary, *Bioceram. Dev. Appl.*, **S**, 1 (2013).
15. C. Gao, Q. Gao, Y. Li, M. N. Rahaman, A. Teramoto and K. Abe, *J. Biomed. Mater. Res. A*, **100**, 1324 (2012).
16. A. Yazdanpanah, R. Kamalian, F. Moztarzadeh, M. Mozafari, R. Ravarian and L. Tayebi, *Ceram. Int.*, **38**, 5007 (2012).
17. S. C. Wong, A. Baji and A. N. Gent, *Compos. Part Appl. Sci. Manuf.*, **39**, 579 (2008).
18. J. R. Jones, *J. Eur. Ceram. Soc.*, **29**, 1275 (2009).
19. R. K. Nalla, J. H. Kinney and R. O. Ritchie, *Biomaterials*, **24**, 3955 (2003).
20. P. Sepulveda, J. R. Jones and L. L. Hench, *J. Biomed. Mater. Res.*, **58**, 734 (2001).
21. T. Peltola, M. Jokinen, H. Rahiala, E. Levänen, J. B. Rosenholm, I. Kangasniemi and A. Yli-Urpo, *J. Biomed. Mater. Res.*, **44**, 12 (1999).
22. M. M. Pereira and L. L. Hench, *J. Sol-Gel Sci. Technol.*, **7**, 59 (1996).
23. R. Li, A. E. Clark and L. L. Hench, *J. Appl. Biomater.*, **2**, 231 (1991).
24. H. Boyar, B. Turan and F. Severcan, *J. Spectrosc.*, **17**, 627 (2003).
25. S. Jebahi, H. Oudadesse, B. Xv, H. Keskes, T. Rebai, A. El Feki and H. El Feki, *Afr. J. Pharm. Pharmacol.*, **6**, 1276 (2012).
26. J. R. Jones, *Acta Biomater.*, **9**, 4457 (2013).
27. S.-H. Shin and H.-I. Kim, *J. Ind. Eng. Chem.*, **7**, 147 (2001).
28. D. Farlay, G. Panczer, C. Rey, P. D. Delmas and G. Boivin, *J. Bone. Miner. Metab.*, **28**, 433 (2010).
29. V. Krishnan and T. Lakshmi, *J. Adv. Pharm. Technol. Res.*, **4**, 78 (2013).
30. Y. Ibn Yacoub, B. Amine, A. Laatiris, F. Wafki, F. Znat and N. Hajjaj-Hassouni, *Rheumatol. Int.*, **32**, 3143 (2012).
31. O. Bretcanu, S. Misra, I. Roy, C. Renghini, F. Fiori, A. R. Boccaccini and V. Salih, *J. Tissue. Eng. Regen. Med.*, **3**, 139 (2009).
32. H. G. Kim and J. H. , *Fibers Polym.*, **12**, 602 (2011).
33. H. Liao, R. Qi, M. Shen, X. Cao, R. Guo, Y. Zhang and X. Shi, *Colloids Surf., B Biointerfaces*, **84**, 528 (2011).
34. M. M. Echezarreta-López and M. Landin, *Int. J. Pharm.*, **453**, 641 (2013).
35. I. Allan, H. Newman and M. Wilson, *Biomaterials*, **22**, 1683 (2001).
36. D. Zhang, O. Leppäranta, E. Munukka, H. Ylänen, M. K. Viljanen, E. Eerola, M. Hupa and L. Hupa, *J. Biomed. Mater. Res. A*, **93**, 475 (2010).
37. H. Nikaido, *J. Bioenerg. Biomembr.*, **25**, 581 (1993).
38. H. Nikaido, *Microbiol. Mol. Biol. Rev. MMBR*, **67**, 593 (2003).